Microglia control the glycinergic but not the GABAergic synapses via prostaglandin E2 in the spinal cord

Yasmine Cantaut-Belarif,[1] Myriam Antri,[2] Rocco Pizzarelli,[1] Sabrina Colasse,[1] Ilaria Vaccari,[1] Sylvia Soares,[3] Marianne Renner,[1] Radhouane Dallel,[2] Antoine Triller,[1] and Alain Bessis[1]

[1]École Normale Supérieure, Institut National de la Santé et de la Recherche Médicale, Centre National de la Recherche Scientifique, Paris Sciences et Lettres Research University, Paris, France
[2]Faculté de Chirurgie Dentaire, Neuro-Dol, Centre Hospitalier Universitaire de Clermont-Ferrand, Université Clermont Auvergne, Institut National de la Santé et de la Recherche Médicale, Clermont-Ferrand, France
[3]Sorbonne Universités, UPMC, CNRS 8246, INSERM 1130, Institut de Biologie Paris-Seine, Neuroscience Paris Seine, Paris, France

Microglia control excitatory synapses, but their role in inhibitory neurotransmission has been less well characterized. Herein, we show that microglia control the strength of glycinergic but not GABAergic synapses via modulation of the diffusion dynamics and synaptic trapping of glycine (GlyR) but not $GABA_A$ receptors. We further demonstrate that microglia regulate the activity-dependent plasticity of glycinergic synapses by tuning the GlyR diffusion trap. This microglia–synapse cross talk requires production of prostaglandin E2 by microglia, leading to the activation of neuronal EP2 receptors and cyclic adenosine monophosphate–dependent protein kinase. Thus, we now provide a link between microglial activation and synaptic dysfunctions, which are common early features of many brain diseases.

Introduction

Microglial cells are immune components of the brain, and their activation has been established as a hallmark of brain pathologies (Ransohoff and Cardona, 2010). However, microglia are also partners of neuronal functions in the healthy brain (Tremblay et al., 2011). In particular, they are implicated in the rapid modulation of excitatory synapses, and microglial stimulations induce specific responses of excitatory neurotransmission (Béchade et al., 2013). For instance, fractalkine activates the microglia-specific CX3CR1 and induces a transient reduction of the amplitude of evoked excitatory postsynaptic currents (PSCs) in CA1 pyramidal neurons (Ragozzino et al., 2006; Clark et al., 2015). Similarly, lipopolysaccharide (LPS), which specifically activates the microglial Toll-like receptor 4, triggers an astrocyte-mediated increase in the frequency of AMPAergic evoked excitatory PSCs (Pascual et al., 2012). Finally, video microscopic analysis of microglia–synapse structural relationships has demonstrated that microglia respond to neuronal activity by modulating the physical contacts between their processes and the excitatory synaptic elements (Wake et al., 2009; Tremblay et al., 2010; Li et al., 2012).

Interactions between microglia and inhibitory synapses have mostly been studied as long-term regulations occurring in pathologies. For instance, during peripheral nerve injury, spinal cord microglia produce brain-derived neurotrophic factor (BDNF), which induces a shift in chloride flux through $GABA_A$ receptors ($GABA_A$Rs) in nociceptive neurons. This leads to an increase of their excitability and contributes to pain hypersensitivity (Coull et al., 2005). Furthermore, long-term activation of microglia may lead to physical deconnections between the pre- and postsynaptic elements of inhibitory synapses (Chen et al., 2014). In addition, immune-derived molecules such as major histocompatibility complex class I molecules (Oliveira et al., 2004) or prostaglandin E2 (PGE2), a major modulator of inflammatory pain (Harvey et al., 2004), regulate inhibitory synapses during diseases. However, microglia are not only actors of pathologies; they may also be involved in acute situations because they are highly dynamic cells that rapidly react to environmental modifications (Davalos et al., 2005; Nimmerjahn et al., 2005). Hence, microglia might also be involved in short-term regulation of inhibitory synapses. This hypothesis is supported by the fact that signaling molecules produced by microglia can rapidly modulate inhibitory synaptic function. For instance, TNF-α induces a rapid decrease of GABAergic synaptic strength associated with a down-regulation of cell-surface $GABA_A$R (Pribiag and Stellwagen, 2013). Similarly, thrombospondin 1 (TSP1), which is also produced by microglia (Chamak et al., 1995), modulates the diffusion dynamic

of GlyR and leads to an increase in its synaptic accumulation (Hennekinne et al., 2013).

We have established that microglia differentially control GABAergic and glycinergic inhibition in the spinal cord. The underlying mechanism is a specific control of the diffusion and subsequent trapping of GlyR but not GABA$_A$R at postsynaptic differentiation. We have identified PGE2 acting via EP2 receptors and protein kinase A as the molecular microglia–neuron intermediary of this regulation.

Results

Short-term microglial stimulation controls inhibitory synapse function by tuning synaptic receptor content

The efficiency of neurotransmission critically depends on the number of receptors accumulated at postsynaptic sites (Choquet and Triller, 2013). As a proof of concept of the rapid regulation of inhibitory synapses by microglia, we first characterized the modulation of GlyR and GABA$_A$R accumulation at synapse upon short-term stimulation of microglia. Stimulation of microglia in vivo was achieved by intrathecal injection of LPS. The effects on GlyR and GABA$_A$R were monitored 30 min after stimulation by quantifying GABA$_A$R γ2 subunit and GlyR α1 subunit immunoreactivities (IRs) at inhibitory synaptic sites identified by gephyrin clusters (Fig. 1, A and B). Stimulation of microglia induced a decrease of synaptic GlyR α1 IR intensity (68 ± 7%; P = 0.021; n = 4; Fig. 1, A and C) but had no effect on synaptic GABA$_A$R IR (84 ± 7%; P = 0.149; n = 4; Fig. 1, B and C). The intensity of the gephyrin clusters associated with GABA$_A$R and GlyR were not modified (115 ± 6% and 111 ± 13%, respectively; P = 0.083 and 0.564, respectively; n = 4). This experiment shows that short-term stimulation of microglia induces a specific decrease of synaptic GlyR but not GABA$_A$R accumulation.

To investigate the impact of this decrease on neurotransmission, whole-cell recordings were performed on substantia gelatinosa neurons in acute spinal dorsal horn slices and spontaneous inhibitory PSCs were analyzed before and after microglial stimulation. In the presence of gabazine, bath application of LPS significantly reduced median glycinergic PSC amplitudes in five out of seven neurons (Fig. 1 D; P = 0.0381; paired *t* test). In contrast, in the presence of strychnine, application of LPS had no significant effect on median GABAergic PSC amplitudes (Fig. 1 E; P = 0.834; paired *t* test; n = 7).

We also investigated the microglia–neuron cross talk in cultured systems. In organotypic slices, microglia conserve their highly branched ramification (Hailer et al., 1996; Hellwig et al., 2013; Fig. S1 A), their electrophysiological properties (De Simoni et al., 2008), and their ability to regulate excitatory synapses (Pascual et al., 2012). As observed in vivo, LPS stimulation of microglia in organotypic slices of spinal cord decreased synaptic GlyR α1 IR (67.3 ± 3.8%; P = 0.0002; n = 10 independent cultures; Fig. S1, B and D) but had no effect on synaptic GABA$_A$R IR (103.4 ± 17.9%; P = 0.513; n = 3) nor on gephyrin IR (91.5 ± 5.0%; P = 0.702; n = 4; Fig. S1, C and D). We also investigated the regulation of inhibitory synapses by microglia in dissociated cultures of spinal cord. In this system, 30-min stimulation of microglia by LPS also induced a decreased accumulation of GlyR α1 IR at gephyrin-positive loci (81.6 ± 4.8%; P = 0.0001; n = 17 independent cultures; Fig. S1,

E and F) but had no effect on gephyrin clusters (114.7 ± 7.1%; P = 0.380; n = 17) or GABA$_A$R IR (101.1 ± 4.6%; P = 0.488; n = 12). As observed in acute slices, the differential regulation of synaptic GABA$_A$R and GlyR accumulation in dissociated cultures was correlated with a significant decrease in the amplitude of spontaneous glycinergic PSCs (Fig. S1, G and H).

In conclusion, these experiments show that microglia can rapidly and differentially modulate GlyR and GABA$_A$R synaptic content (SC) by a mechanism that is conserved from in vivo spinal cord to dissociated cells. This modulation correlates with a differential modulation of GABAergic and glycinergic neurotransmission.

Microglia controls GlyR but not GABA$_A$R synaptic trapping through a lateral diffusion–dependent mechanism

Diffusion trap is important for the regulation of the receptor number at synapses (Choquet and Triller, 2013). We thus examined how microglial cells control the lateral diffusion of GABA$_A$R and GlyR. The surface mobility of neurotransmitter receptors has mostly been studied in cell cultures using specific antibodies coupled to quantum dots (QDs) in single-particle tracking experiments (Bannai et al., 2006). We tracked the dynamic behavior of endogenous GlyR α1 and GABA$_A$R γ2 in dissociated cultures of spinal cord using QDs. Consistent with previous studies (Charrier et al., 2010; Hennekinne et al., 2013), a pool of "stable" receptors remained at mRFP–gephyrin–positive synapses during the recording session, whereas a pool of "mobile" receptors swapped between synaptic and extrasynaptic compartments (Fig. 2 A). Fine tuning of synaptic receptor content can be achieved by regulating these two pools of receptors. We analyzed the action of microglia on the dynamic behavior of stable and swapping GlyR and GABA$_A$R, respectively. First, we established that the stimulation of microglia had no effect on the diffusion coefficients of extrasynaptic GABA$_A$R and GlyR as well as on the stable synaptic receptors (Fig. S2, A–D). Then, we found that swapping GlyR, but not GABA$_A$R, slowed down after the stimulation of microglia (Fig. S2, C and D). Similarly, the stimulation of microglia specifically increased the synaptic area explored by GlyR but not that of GABA$_A$R (Fig. 2 B) and had no effect on the extrasynaptic area explored by GABA$_A$R and GlyR (Fig. 2 C). The short-term stimulation of microglial cells also differentially tuned the dynamic stability of GABA$_A$R and GlyR at synapses (Fig. 2, E and F). Indeed, GlyR synaptic dwell times shifted toward lower values, and the pool of stable synaptic GlyR decreased (from 47.3 ± 2.5% to 40.0 ± 2.7%; P = 0.026; n = 4; *t* test; Fig. 2 E), whereas GABA$_A$R γ2 synaptic stability was not affected (Fig. 2 F).

Rapid tuning of synaptic receptor content by lateral diffusion results not only from the regulation of the stability of receptors at synapses but also from changes of receptors' capacity to switch from extrasynaptic to synaptic sites. We thus monitored how microglia modulated the swapping properties of GABA$_A$R and GlyR (Fig. 3 and Fig. S2 E). To approach this issue, we computed for each field the proportion of receptor QDs at mRFP–gephyrin clusters as a function of time (Fig. 2 A and Fig. S2 E). The receptor QDs trapped at synapses during the whole recording session, as well as the one remaining at extrasynaptic sites, were excluded from the analysis. The SC of swapping GABA$_A$R QDs and GlyR QDs was defined by the number of receptor QDs divided by the number of mRFP–gephyrin clusters. It was then quantified during the recording sessions (Fig. S2 E)
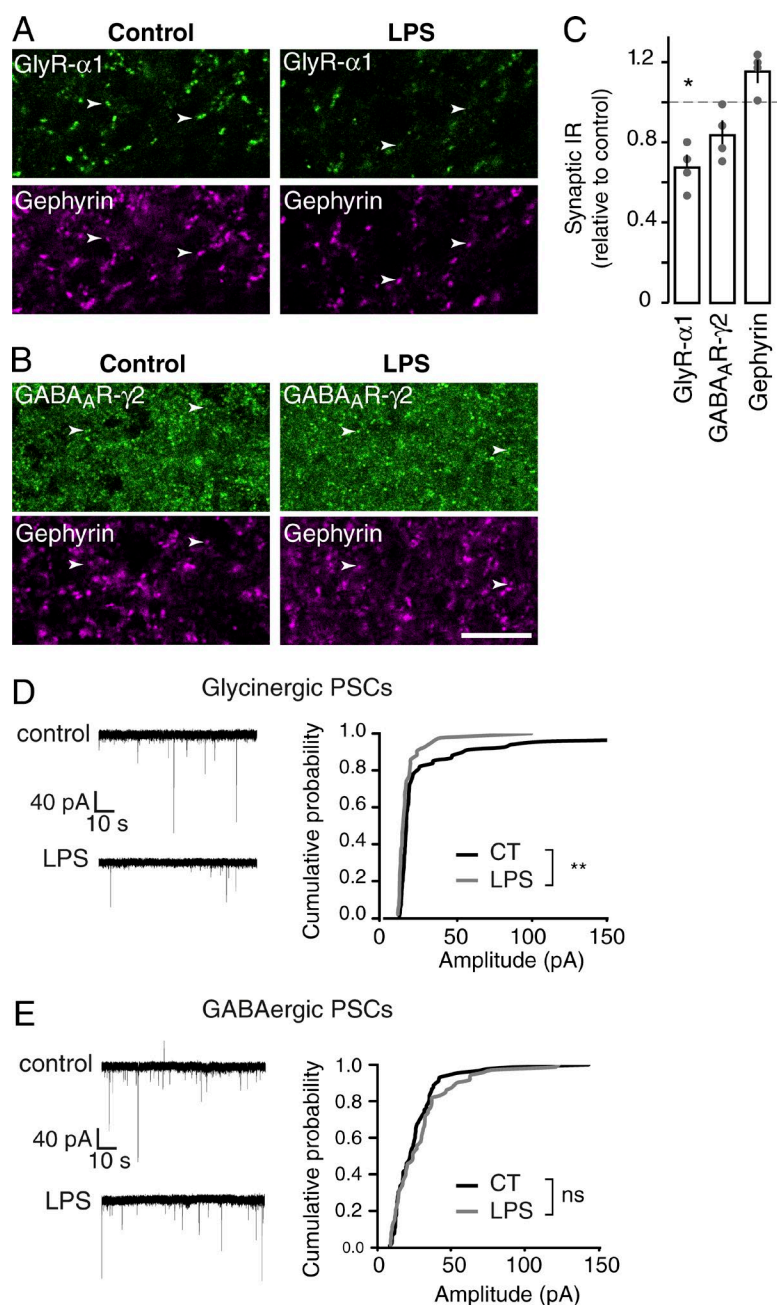
Figure 1. **Short-term stimulation of microglia specifically decreases GlyR synaptic accumulation and spontaneous glycinergic PSCs.** (A and B) Double detection of GlyR α1 IR (A) and GABA$_A$R γ2-IR (B, top) with postsynaptic marker gephyrin (bottom) in the dorsal horn of thoracic spinal cord 30 min after intrathecal injection of vehicle (left) or LPS (right). Arrowheads show clusters of receptors colocalizing with gephyrin clusters. Bar, 10 μm. (C) Quantitative analysis of synaptic GlyR α1 IR and GABA$_A$R γ2 IR colocalized with gephyrin IR in the dorsal horn 30 min after LPS injection. Data are expressed as a percentage of fluorescence intensity in control condition (dotted line). Circles represent single animals. *, P = 0.0209; Mann-Whitney test. (D and E) Representative traces (left) and cumulative histogram of amplitudes (right) of spontaneous glycinergic (D) and GABAergic (E) PSCs recorded from substantia gelatinosa neurons in control conditions and after LPS application. Amplitudes in cumulative graphs are recorded from the same neurons in control conditions (black) and after LPS application (gray). **, P < 0.01; Kolmogorov-Smirnov test.

in control conditions and after microglial stimulation. The system was at a steady state because the SC of swapping GABA$_A$R QDs and GlyR QDs remained stable during the recording session (Fig. 3, A and B). However, when microglia were stimulated, the SC of swapping GlyR QDs was reduced to 64.3 ± 0.1% of the control (P < 0.001; *t* test; Fig. 3 A), whereas that of swapping GABA$_A$R at synapses was significantly but barely affected (103.7 ± 0.2%; P < 0.001; *t* test; Fig. 3 B). Accordingly, short-term stimulation of microglia decreased the frequency of transitions between synaptic and extrasynaptic GlyR QDs from 0.16 ± 0.01 to 0.12 ± 0.01 Hz (P = 0.009; *t* test) but had no effect on the frequency of GABA$_A$R QD transition (Fig. 3, C and D). The rapid modulations of synaptic receptor content occur through lateral diffusion of receptors rather than by membrane insertion of new receptors. Indeed, surface biotinylation assays indicated that, as expected, stimulation of microglia did not

change the proportion of GlyR α1 and GABA$_A$R γ2 being incorporated in the plasma membrane (Fig. 3, E and F).

In conclusion, stimulation of microglia in the spinal cord rapidly modifies the membrane diffusion properties of GlyR, leading to a destabilization of synaptic GlyR at synapses and a tendency to leave the synaptic site. It results in a reduction of the GlyR SC and decreased glycinergic PSCs. In contrast, stimulation of microglial cells does not affect the diffusion dynamic and synaptic stability of GABA$_A$R and has no effect on the number of synaptic GABA$_A$R or GABAergic PSCs.

Microglia control the homeostatic regulation of synaptic glycine receptor trapping

Modulation of synaptic receptor content plays a role in synaptic scaling, in which the number of receptors at synapse is adapted
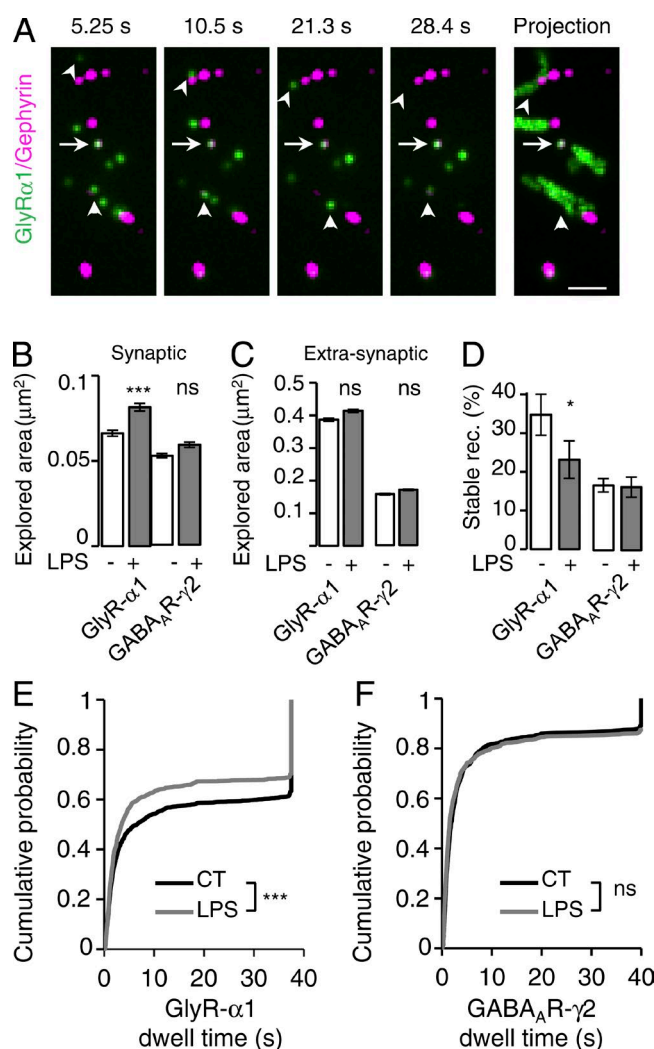
Figure 2. Microglia tune GlyR but not GABA_AR synaptic stability through lateral diffusion. (A) Representative time-lapse recording of GlyR α1 QDs (green) and mRFP–gephyrin fluorescent domains (purple). A maximum intensity projection of 500 frames recorded at 13 Hz is also shown (right). Stable GlyR α1 QDs stay at mRFP–gephyrin synapses during the whole recording session (arrows). Mobile GlyR α1 QDs (arrows) swapped between synaptic and extrasynaptic compartments. Bar, 1 µm. (B and C) Explored area of synaptic (B) and extrasynaptic (C) receptors in control (white) and after LPS application (gray). $n = 4$ and 5 independent cultures for GlyR α1 IR and GABA_AR γ2 IR, respectively. Mean ± SEM; ***, $P < 0.001$; t test. (D) Percentage of stable synaptic receptors detected during the imaging session. Mean ± SEM; *, $P < 0.05$; t test). (E and F) Synaptic dwell time distributions in control (black) and after LPS application (gray). GlyR: $n_{CT} = 1,384$ and $n_{LPS} = 1,130$ trajectories. GABA_AR: $n_{CT} = 795$ and $n_{LPS} = 909$ trajectories. ns, $P > 0.05$; ***, $P < 0.001$; Kolmogorov-Smirnov test.

to compensate for modification of neuronal activity (Kilman et al., 2002; Stellwagen and Malenka, 2006). In organotypic slices as well as in dissociated cultured cells from the spinal cord, application of 4-aminopyridine (4AP) induced an adaptive decrease of the synaptic GlyR α1 IR with no change in the GABA_AR γ2 IR (organotypic slices + 4AP: synaptic GlyR α1 IR: $73.0 ± 4.0\%$ of control; $P = 0.001$; $n = 4$; synaptic GABA_AR γ2 IR: $92.4 ± 4.9\%$ of control; $P = 0.05$; $n = 3$; gephyrin IR: $105.3 ± 4.4\%$ of control; $P = 0.248$; $n = 4$; Fig. 4; dissociated cultures + 4AP: synaptic GlyR α1 IR: $74.1 ± 5.3\%$ of control; $P < 0.001$; $n = 15$; synaptic GABA_AR γ2: $102.1 ± 5.8\%$ of control; $P = 0.400$;

$n = 8$; mRFP–gephyrin: $112.8 ± 9.9\%$ of control; $P = 0.713$; $n = 13$; Fig. S3, A and B).

To test the involvement of GlyR lateral diffusion in this regulation, we cross-linked the cell-surface GlyR using primary antibodies targeting extracellular epitopes and thus specifically impeded their lateral mobility as previously performed for other membrane receptors (Renner et al., 2010; Murphy-Royal et al., 2015). As expected, this procedure dramatically decreased the GlyR diffusion coefficient, and increased their confinement (Fig. S4, B–D), thereby decreasing their availability to diffuse in and out of synapses. When GlyR cross-linking was achieved before 4AP application, it precluded the effect of activity on the SC of GlyR (cross-linking + 4AP: $93.9 ± 8.7\%$ of cross-link; $P = 0.513$; $n = 3$). This result demonstrates that the plastic regulation of synaptic GlyR content depends on GlyR lateral mobility. Because GlyR lateral diffusion is also controlled by microglia, we hypothesized that microglia can thereby tune the adaptive modulation of GlyR accumulation at synapses. Indeed, when microglial cells were stimulated by LPS, a subsequent application of 4AP did not further decrease the SC of GlyR (organotypic slices, Fig. 4 A: LPS + 4AP: $62.0 ± 7.2\%$ of control; $P = 0.002$; $n = 6$; LPS + 4AP vs. LPS: $P = 0.680$; dissociated cultures, Fig. S3 A: LPS + 4AP: $75.7 ± 5.9\%$ of control; $P = 0.001$; $n = 12$; difference between LPS + 4AP and LPS: $P = 0.862$). The consequences of microglial stimulation and modulation of neuronal activity on the synaptic GlyR are thus not additive content, suggesting that they share the same regulatory pathway.

We also directly analyzed the involvement of microglia in the homeostatic control of GlyR at synapses. To this end, we depleted microglial cells from neuronal cultures using the microglia-specific immunotoxin Mac1-saporin and examined the effects on the activity-dependent regulation of synaptic GlyR (Fig. S5). Putative nonspecific effects were ruled out by showing that depletion did not modify the synaptic localization of GlyR and GABA_AR clusters nor the density of synapses or the proportion of glycinergic and GABAergic synapses (Fig. S5 B). We further verified that after depletion of microglia, application of LPS onto the culture had no further effects on the lateral mobility of GlyR and GABA_AR (Fig. S5 D). Strikingly, when neuronal cultures were depleted from microglia, 4AP depolarization had no effect on the synaptic accumulation of GlyR (synaptic GlyR α1: $111.2 ± 15.0\%$ of control; $P = 0.248$; $n = 4$). Thus, these experiments demonstrate that microglia are necessary for the activity-dependent regulation of the SC of GlyR.

PGE2 mediates the microglial modulation of synaptic GlyR

We then investigated the molecular mediator potentially involved in the regulation of inhibitory synapses by microglia. The differential regulation of GlyR and GABA_AR by microglia that we observed is reminiscent of the selective blockade of glycinergic neurotransmission by PGE2 acting on neuronal EP2 receptors (Ahmadi et al., 2002; Reinold et al., 2005). Because PGE2 is specifically produced by microglia upon LPS stimulation (Ikeda-Matsuo et al., 2005), we tested the involvement of PGE2 and EP2 receptors (EP2Rs) in the microglia- and activity-dependent accumulation, stabilization, and trapping of GlyR at synapses. We first showed that in spinal cord organotypic slices, the expression of Cox-2, the rate-limiting enzyme of PGE2 synthesis, is restricted to microglia (Fig. 5 A), as shown by the strong correlation between anti-Cox-2 and anti-Iba1 immunostaining (Pearson
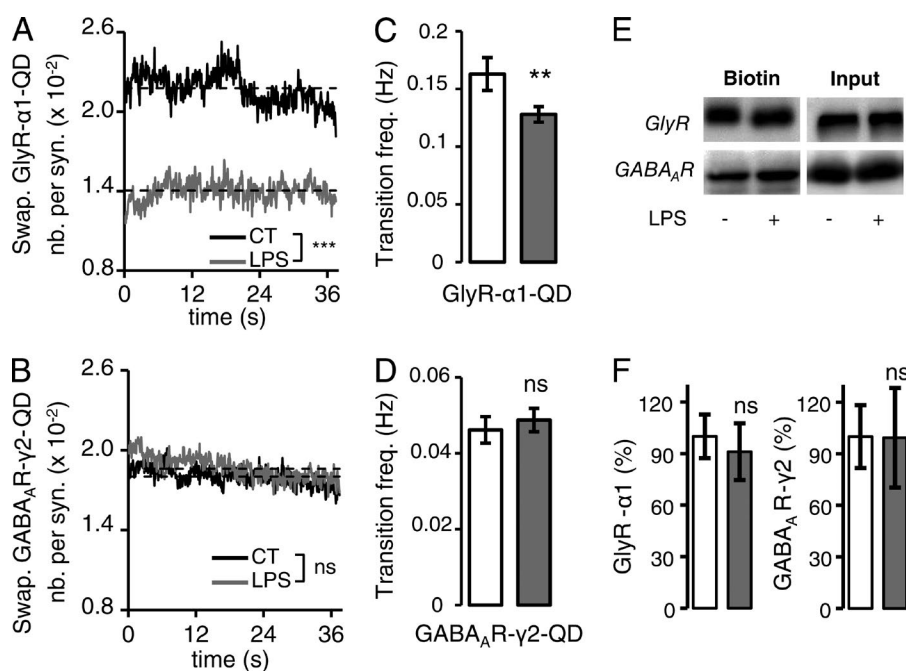
Figure 3. **Short-term stimulation of microglia decreases the proportion of synaptic swapping trajectories.** (A and B) SC of swapping GlyR α1 (A) and GABA$_A$R γ2 (B) in control (black) and after LPS application (gray). (C and D). Transition frequency of GlyR α1 QDs (C) and GABA$_A$R γ2 QDs (D) in and out of the synapses. Mean ± SEM; ns, P > 0.05; **, P < 0.01; *t* test. (E) Representative Western blots of GlyR α1 and GABA$_A$R γ2 in the total amount of protein (input) or in the biotinylated fraction at the cell surface (biotin) in control of LPS-treated cells. (F) Mean ratio (±SEM) of surface-to-total GABA$_A$R γ2 and GlyR α1 levels in control condition (white) and after LPS application (gray). Data are expressed as a percentage of control (*n* = 5 and 4 cultures, respectively; ns, P > 0.05; *t* test).

coefficient 0.69 ± 0.04; *n* = 3 independent slice cultures). In addition, upon modulation of neuronal activity or stimulation of microglia, Cox-2 IR significantly increased (fold increase of Cox-2 IR: 3.3 ± 0.7 and 3.9 ± 1.3 between control and 4AP- and LPS-treated organotypic slices, respectively; P = 0.049; Mann-Whitney U test; *n* = 3 independent slice cultures; Fig. 5 B) but was still restricted to microglia (Pearson correlation coefficient between Cox-2 and Iba1 IR: 0.76 ± 0.04 and 0.74 ± 0.04 upon 4AP and LPS application, respectively). We then confirmed that EP2R is expressed mostly by neurons, as previously demonstrated (Bilak et al., 2004; Zhao et al., 2007; Liang et al., 2008; Fig. S5 A).

Then, we characterized the involvement of EP2R in this acute microglial-dependent regulation of synaptic GlyR. As a first approach, we tested the involvement of EP2R using pharmacology rather than gene knockout to overcome potential indirect effects caused by compensatory mechanisms or developmental reorganization. Application of the specific antagonist of EP2R, PF04418948 (PF044; Forselles et al., 2011), prevented the decrease of GlyR synaptic dwell time and of the proportion of stable receptors induced by LPS stimulation (Fig. 5, C and D; and Fig. S5 B). It also prevented the decreased accumulation of GlyR at synapses in organotypic slices (LPS + PF044: 91.3 ± 19.7% of control; P = 0.248; *n* = 4; Fig. 5 E) and in cultured neurons (LPS + PF044: 102.6 ± 5.8% of control; P = 0.773; *n* = 4; Fig. S5, B and C). Blocking EP2 receptors also abolished the regulation of synaptic GlyR induced by 4AP in organotypic slices (4AP + PF044: 91.2 ± 4.1% of control; P = 0.050; *n* = 3; Fig. 5 E) and in dissociated cultures (87.8 ± 17.3% of control; P = 0.564; *n* = 4; Fig. S5 C).

To gain insight into the mechanism of this regulation, we tested the involvement of the cAMP-dependent protein kinase (PKA), which has previously been shown to be required for the regulation of GlyR by PGE2 (Ahmadi et al., 2002). Fig. 5 F shows that blocking PKA activity with H-89 prevented the decreased accumulation of GlyR induced by the stimulation of microglia (application of LPS: 115.7 ± 12.6% of control; P = 0.2882; *n* = 4) as well as the activity-dependent adaptive modu-

lation of synaptic GlyR (application of 4AP: 109.3 ± 17.8% of control; P = 1; *n* = 4).

In conclusion, these experiments demonstrated that microglia control the homeostatic regulation of synaptic GlyR content though PGE2 acting on neuronal EP2 receptors via PKA.

Discussion

Microglia are the most dynamic cells of the brain parenchyma; they detect and react instantaneously to subtle modifications of their environment. Initially described as actors of brain pathologies (Kreutzberg, 1996), they are now acknowledged as key partners of neuronal function in the healthy brain (Tremblay et al., 2011; Béchade et al., 2013). Our work now deepens this concept and reveals that microglia achieve acute and rapid control of glycinergic neurotransmission by PGE2-dependent control of GlyR lateral diffusion and synaptic accumulation.

Microglia rapidly modulate the SC of glycine but not of GABA$_A$Rs and regulate inhibitory synaptic strength

We first established that microglia can modulate inhibitory synaptic function. Deciphering the role of glial cells critically depends on the possibility of specifically blocking or stimulating their functions. In this study, as a proof of concept, we stimulated microglial cells using LPS. It has been extensively demonstrated that in nervous tissue, TLR4, which is the LPS receptor, is only expressed by microglia (Lehnardt et al., 2003; Chakravarty and Herkenham, 2005; Holm et al., 2012; Pascual et al., 2012). Therefore, LPS allowed us to describe the synaptic effects of the specific stimulation of microglia. Stimulation of microglia was shown to significantly reduce the synaptic accumulation of GlyR but not GABA$_A$R and, as a result, it decreased the amplitude of spontaneous glycinergic but not GABAergic PSCs. Thus, these experiments revealed a functional link between microglia and inhibitory synapses.
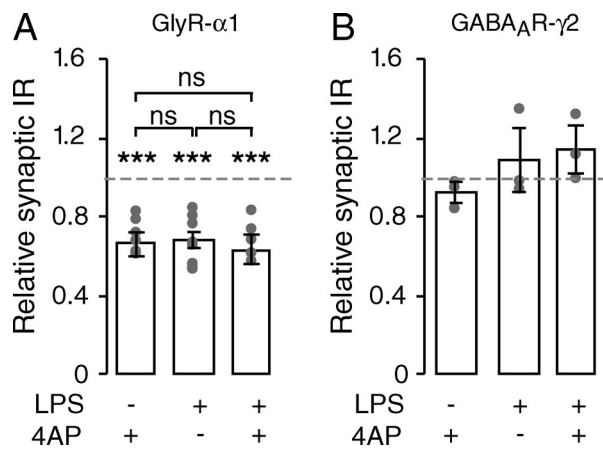
Figure 4. The adaptive plastic regulation of GlyR is modulated by microglia. Fluorescence intensities relative to control (mean ± SEM) of synaptic GlyR α1 IR (A) and GABA$_A$R γ2 IR (B) after 15-min application of 4AP preceded (or not) by 30-min LPS stimulation of microglia in organotypic slices of spinal cords. The effects of 4AP and LPS treatments are not additive. Circles represent single cultures; ns, P > 0.05; ***, P < 0.001; Mann-Whitney test.

The same differential regulation of inhibitory receptors occurred in vivo after intrathecal injection of LPS, ex vivo in organotypic slices, and in vitro in dissociated cultured cells upon application of LPS. In organotypic slices, microglia are surrounded by neurons and astrocytes, and they conserve their ramified morphology (Hailer et al., 1996), their electrophysiological properties (De Simoni et al., 2008), and their ability to regulate excitatory synapses (Pascual et al., 2012). This suggests that—at least for these properties—they retain a phenotype similar to that of microglia in situ. Thus, regulatory interactions between neurons and microglia are likely to be conserved in organotypic slices. The morphology of microglial cells is modified in dissociated cell cultures. Most of their physical interactions are lost, but not all their functions are altered (Hellwig et al., 2013). Indeed, cultures have often been used to successfully explore regulatory interactions between neurons and glial cells (Saijo et al., 2009; Pascual et al., 2012; Wang et al., 2015). Our results now demonstrate that the microglia–neuron interactions regulating the inhibitory synapses are conserved from in vivo to in vitro models.

Microglia tune the synaptic accumulation and lateral diffusion of GlyR

In physiological conditions, neurotransmitter receptors are permanently exchanged between synaptic and extrasynaptic sites (Dahan et al., 2003). Such permanent exchange leads to a dynamic equilibrium that sets the number of synaptic receptors at a steady state. This equilibrium depends on diffusion parameters such as dwell time and confinement at synapse or diffusion coefficients. It also depends on physical constraints and protein–protein interactions (Choquet and Triller, 2013). As a result, the number of receptors that accumulate at synapses depends on a combination of dynamic and physical factors that are highly interdependent. When a plastic adaptation of the PSC is needed, the equilibrium of synaptic versus extrasynaptic receptors can be quickly shifted to another set point by tuning the diffusion trap of receptors. This results in a rapid adaptation of the number of receptors at synapses and hence a rapid adaptation of the synaptic response.

Microglia have been suggested to be involved in the plastic regulation of synaptic activity based on the observation that a loss of function of microglial signaling membrane proteins such as DAP12, CX3CR1, or CD200 leads to impaired long-term potentiation in the hippocampus (Roumier et al., 2004; Costello et al., 2011; Rogers et al., 2011). We now have established that microglia tune the dynamic equilibrium of synaptic versus extrasynaptic GlyR by modulating the synaptic dwell time as well as the speed and the entrance/exit frequency of swapping synaptic GlyR. We have further shown that microglia control the activity-dependent plasticity of synaptic GlyR. More precisely, a decrease in neuronal activity induces an adaptive diffusion-dependent reduction of synaptic GlyR (Lévi et al., 2008). When the microglial cells are depleted or stimulated before the change in neuronal activity, the diffusion properties of GlyR are modified and the new dynamic equilibrium cannot be reached, thus preventing the adaptive regulation.

We found that microglia did not acutely regulate GABA$_A$R. This work was performed in the spinal cord in which the GABAergic and glycinergic transmissions coexist. In this system, the differential GABA$_A$R/GlyR modulation is likely to allow maintenance of global inhibition through the glycinergic component and smaller adjustments through the GABAergic one. One may speculate that microglia regulate inhibitory neurotransmission through different mechanisms in the rostral regions of the nervous system in which inhibitory transmission is mostly, if not exclusively, GABAergic (Freund and Buzsáki, 1996). Depletion of microglia from the brain has also been shown to alter the function of glutamatergic synapses (Parkhurst et al., 2013), suggesting that microglia may provide a coordinated regulation of excitation inhibition within neuronal networks. Indeed, microglial cells are particularly dynamic and reactive to modifications of the brain parenchyma physiology. By modulating the strength and plasticity of excitatory and inhibitory synapses, microglia are thus constantly and rapidly adapting the activity of the neuronal network to the local environment.

Regulation of inhibitory synapses by microglia is mediated by PGE2

We found that the stimulation of microglia by LPS modulates the lateral mobility of GlyR, decreases the accumulation of GlyR at synapses, and reduces the amplitude of glycinergic PSCs, but has no effect on GABA$_A$R. This latter effect is similar to the effect of PGE2, which induces a selective decrease of glycinergic PSC without impairing the GABAergic PSCs (Ahmadi et al., 2002). In nervous tissue, PGE2 can be produced by microglia but can also be produced by neurons and astrocytes (Samad et al., 2001; Ikeda-Matsuo et al., 2005; Clasadonte et al., 2011). Therefore, the regulation of synaptic function by microglia could involve other cell types, as previously demonstrated for excitatory synapses (Pascual et al., 2012). However, we have shown that upon LPS stimulation of microglia or 4AP-induced modulation of neuronal activity, Cox-2, which is the rate-limiting PGE2 synthesizing enzyme, is only up-regulated in microglia (Ikeda-Matsuo et al., 2005). Therefore, the regulation of glycinergic synapses that we have unveiled is most likely a result of PGE2 produced by microglia. We have further shown that blocking the PGE2 EP2 receptor prevents the effect of microglial stimulation on the mobility and synaptic accumulation of GlyR, and above all it hampers the microglial-dependent homeostatic regulation of synaptic GlyR. In the spinal cord, EP2R has
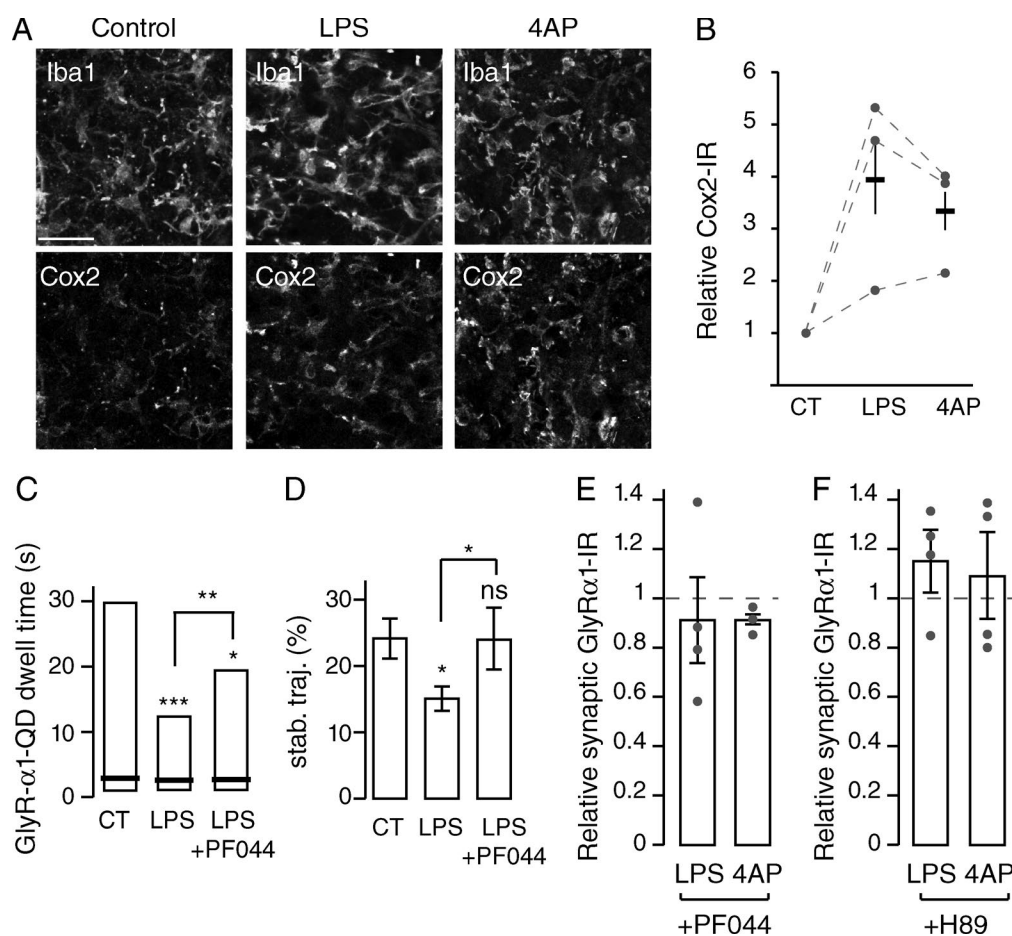
Figure 5. **PGE2 mediates microglial regulation of synaptic GlyR accumulation via EP2 receptors.** (A) Double labeling of organotypic slices showing Cox-2 and Iba1 IRs in control condition and after 30-min LPS application or 15-min 4AP application. Cox-2 IR is restricted to microglia. Bar, 20 µm. (B) Quantification (mean ± SEM) of Cox-2 fluorescence intensities over the corresponding Iba1 profiles in control (CT), LPS, and 4AP conditions. Circles represent single experiments. (C and D) The modulation of GlyR α1 QD synaptic dwell time (C) and stability (D) in control (CT), after LPS application (LPS), and after LPS and PF04418948 treatment (LPS + PF044). (C) Synaptic dwell time distributions indicating 25, 50 (black bar), and 75% of all trajectories. *, P < 0.05; **, P < 0.01; ***, P < 0.001; Kolmogorov-Smirnov test. (D) Percentage of stable synaptic trajectories detected during the imaging session (n = 3 independent experiments; mean ± SEM; ns, P > 0.05; *, P < 0.05; t test). (E and F) Fluorescence intensities relative to control of synaptic GlyR α1 IR after application of LPS or 4AP in the presence of EP2 receptor antagonist PF04418948 (E) or the PKA antagonist H-89 (F) in organotypic slices. Mean ± SEM; circles represent single experiments.

been detected mostly in neurons (Bilak et al., 2004; Zhao et al., 2007; Liang et al., 2008). Therefore, our data favor a model in which microglia produce PGE2 that binds to neuronal EP2R and modulates the GlyR diffusion trap properties at synapses. The initial demonstration of a down-regulation of glycinergic currents by PGE2 (Ahmadi et al., 2002) could be reconstituted in GlyR- and EP2R-transfected HEK293 cells upon bath application of glycine (Harvey et al., 2004). In this system, there is no synapse and the modulation of lateral diffusion of GlyR cannot be tracked. Therefore, the regulation that we have discovered represents a new pathway for the modulation of GlyR by PGE2.

We also found that microglia induced a prostaglandin-dependent destabilization of synaptic GlyR with no change in the number of receptors at the cell surface. The destabilization of GlyR could result from a reduced number of accessible gephyrin molecules and/or from decreased interactions among gephyrin, receptors, or the cytoskeleton. Because the stimulation of microglia had no effect on gephyrin accumulation, the destabilization of synaptic GlyR likely results from a decrease of the binding of GlyR to gephyrin. It has been shown that phos-

phorylations of GlyR shape their interaction with gephyrin and thereby their dynamic behavior (Specht et al., 2011). Actually, PGE2 binding to EP2 receptors activates cAMP–PKA signaling (Jiang and Dingledine, 2013). The regulation of GlyR lateral diffusion by PKA has not yet been specifically addressed, but PKA has been shown to regulate GlyR currents (Ren et al., 1998; Ahmadi et al., 2002; Harvey et al., 2004). The differential regulation of GABAergic and glycinergic neurotransmission by microglia could occur through a differential PGE2-triggered PKA phosphorylation of GABA$_A$R and GlyR. Previous regulation of GlyR by PGE2 has been demonstrated to occur on α3 subunits containing GlyR (Harvey et al., 2004). In this study, we show that synaptic α1-containing GlyR is modulated by PGE2. These results, however, are not contradictory because both subunits can be detected within the same synaptic clusters (Harvey et al., 2004) and may be contained in the same GlyR pentamers. In that case, our results would target a subpopulation of GlyR containing both α1 and α3 subunits.

Our work reveals that PGE2 is an effector of microglia-dependent regulation of synaptic function. Other microglial molecules are known to modulate synaptic function. For

instance, in the spinal cord, thrombospondin-1 reduces the synaptic accumulation of AMPA receptors and increases that of GlyR (Hennekinne et al., 2013). In addition, this effect is counteracted by TNF, which is also produced by microglia (Berta et al., 2014). Furthermore, TNF mediates the scaling of synaptic activity during the blockade of neuronal activity by modulating the membrane expression of AMPA and $GABA_A$R in the hippocampus (Stellwagen and Malenka, 2006). Thus, microglia are involved in the regulation of several aspects of synaptic function.

In the pain field, microglia have been mostly involved in causing neuropathic pain, but recent evidence suggests that they might also contribute to inflammatory pain (Berta et al., 2014; Ji et al., 2014). In addition, prostaglandins and cyclooxygenases appear to play a significant role in inflammatory pain (Broom et al., 2004; Reinold et al., 2005). Therefore, the destabilization of GlyR by microglial prostaglandin reported in the present study could be an early step in this pathological process. More generally, our data significantly extend the understanding of glial functions by showing that microglia are actively regulating inhibitory synapses. We have discovered a novel dimension of the regulation of the excitation/inhibition balance, which is not only altered in pathological situations such as pain but is also altered in epilepsy or sensory deprivation processes that are known to involve microglia (Basbaum et al., 2009; Tremblay et al., 2010; Ferrini and De Koninck, 2013).

Materials and methods

Animals
All experiments were approved by the Charles Darwin Ethical Committee (Ce5-2014-001 and 1339-2015073113467359).

Spinal cord slices, cell cultures, and pharmacology
Spinal cords from P3–P7 C57BL/6 mice were sliced using a McIllwain tissue chopper (Mickle Laboratory). Slices (200 µm) were placed on Millicell CM inserts (Millipore) and maintained for 14 to 21 d in MEM supplemented with 20% heat-inactivated horse serum, 2 mM L-glutamine, 1 mM $CaCl_2$, 2 mM $MgSO_4$, 2 mM $MgCl_2$, 11 mM D-glucose, 5 mM $NaHCO_3$, and 20 mM Hepes.

Primary cultures of spinal cord neurons were prepared from C57Bl6/J or mRFP–gephyrin knockin mice at E13 as described previously (Specht et al., 2011) and plated at 2.4 10^4 cells/cm^2 in Neurobasal medium (Invitrogen) supplemented with B27 (Invitrogen), 2 mM glutamine, 5 U/ml penicillin, and 5 µg/ml streptomycin. Spinal cord neurons were used between 14 and 19 d in vitro.

Stimulation of microglial activity was achieved using 30-min application of LPS (InvivoGen) at 50 ng/ml (spinal cord cultures) and 500 ng/ml (intrathecal injection; organotypic slices). In both cases, control conditions refer to an application of vehicle (PBS) solution. Microglia depletion was performed at 11 d in vitro by 72-h application of the immunotargeted toxin CD11b-saporin (0.35 µg/ml; Mac1-Sap; Advanced Targeting Systems). The potassium channel blocker 4AP (Tocris) was applied at 50 µM for 15 min. PF04418948 (Cayman Chemical) was used at 300 and 30 ng/ml for 30 min on organotypic slices and dissociated cell cultures, respectively. The PKA inhibitor H-89 (Sigma) was used at 20 µM.

For cross-linking experiments, cells were incubated for 10 min at 37°C with a laboratory-made rabbit anti-GlyR α1 antibody targeting an extracellular epitope (dilution 1:20).

Immunofluorescence labeling, imaging, and analysis
Adult C57Bl6/J mice were intrathecally injected with 5 µl of LPS or vehicle (PBS) solution and perfused with 4% PFA. Spinal cords were dissected out, postfixed in 4% PFA, cryoprotected in 20% sucrose, and processed for cryosection (18 µm). For each condition, we analyzed $n = 4$ animals (two females and two males). For each animal and for each experimental condition, we analyzed eight thoracic-to-lumbar spinal cord slices. For each slice, one image was acquired. One image is a 2-µm stack of four confocal slices.

Organotypic slices were fixed in 2% or 4% PFA. Slices were permeabilized and blocked in PBS 0.1% Triton X-100 and 0.25% fish gelatin and incubated with primary antibodies (anti-GlyR α1 [1:400; rabbit]; anti-$GABA_A$R γ2 [1:50; Alomone Labs], anti-gephyrin [1:400; mAb7a; Synaptic Systems], anti-Cox-2 [1:200; M-19; Santa Cruz Biotechnology], anti-Iba1 [1:400; Wako], and anti-EP2R [Alomone Labs]). Imaging was performed using a TCS SP5 or SP8 confocal microscope (Leica Microsystems). For each condition, we performed $n = 3$–16 independent cultures. In each culture and for each experimental condition, we analyzed three to four independent slices. For each slice, four to six images were acquired in the dorsal horn. One image is a 2-µm stack of four confocal slices.

Cultured cells were fixed with 90% cold methanol at −20°C for double immunodetection of GlyR and $GABA_A$R or fixed with 4% PFA for single immunodetection of inhibitory receptors. Cells were permeabilized with 0.1% Triton X-100 when required and blocked with 0.25% fish gelatin. Immunolabeling of synaptic receptors was performed in 0.25% fish gelatin using anti-GlyR α1 (1:800; mAb2b; Synaptic Systems) and $GABA_A$R γ2 (1:100; Alomone Labs). Imaging was performed using a confocal spinning disk microscope (DM5000B [Leica Microsystems]; spinning disk head CSU10 [Yokogawa]). For each condition, we performed $n = 5$–17 independent cultures. For each culture and for each experimental condition, we analyzed duplicate coverslips. In each coverslip, 8–12 images were randomly acquired. One image is a single confocal slice.

The synaptic localization of gephyrin clusters has previously been demonstrated in mature cultures of spinal cord neurons (Hanus et al., 2006). We further showed that in the spinal cord, gephyrin clusters are apposed to vesicular GABA transporter (VGAT) puncta (Fig. S5). Therefore, endogenous mRFP–gephyrin or gephyrin IR clusters were used as synaptic markers as described previously (Specht et al., 2011). A cluster was defined as synaptic when it contained at least one pixel colocalized with gephyrin fluorescence. The fluorescence intensities of $GABA_A$R or GlyR clusters colocalized with mRFP–gephyrin or gephyrin IR were quantified using homemade software in MATLAB as previously described (Shrivastava et al., 2015). In brief, images were filtered by wavelet decomposition to generate background-free masks showing clusters of $GABA_A$R, GlyR, or gephyrin. These masks were used to identify the clusters of $GABA_A$R or GlyR that were completely or partially colocalizing with gephyrin. These clusters were characterized as synaptic. The total fluorescence intensity of synaptic clusters was then quantified on the original images. The same procedure was used to quantify the gephyrin clusters apposed to VGAT or Cox-2 IR colocalized with Iba1 IR. Quantification of Pearson correlation was calculated with Icy software using the Colocalization studio plugin (Lagache et al., 2015).

Whole-cell patch-clamp recordings
Acute slices. Mice (C57BL/6; both sexes, aged 21–37 d) were anaesthetized with an intraperitoneal overdose of chloral hydrate (7%). A laminectomy was performed to remove the spinal cord in an ice-cold sucrose-based saline solution containing 2 mM KCl, 0.5 mM $CaCl_2$, 7 mM $MgCl_2$, 1.15 mM NaH_2PO_4, 26 mM $NaHCO_3$, 11 mM glucose, and 205 mM sucrose. Transverse slices (350 µm) of the tho-

racolumbar spine (T11–L3) were cut with a vibratome (VT1200 S; Leica Microsystems) and incubated at 37°C in artificial cerebrospinal fluid containing 130 mM NaCl, 3 mM KCl, 2.5 mM CaCl$_2$, 1.3 mM MgSO$_4$, 0.6 mM NaH$_2$PO$_4$, 25 mM NaHCO$_3$, and 10 mM glucose, pH 7.4, bubbled with 95% O$_2$ and 5% CO$_2$ for a 45-min recovery period before electrophysiological recordings. Substantia gelatinosa neurons were recorded with patch pipettes (5–7 MΩ resistance) filled with an internal solution containing 145 mM KCl, 5 mM EGTA, 2 mM MgCl$_2$, 10 mM Hepes, 2 mM ATP-Na$_2$, 0.2 mM GTP-Na$_2$ neurobiotin (0.05%; Vector Laboratories), and dextran tetramethylrhodamine (10,000 MW; fluoro-ruby; 0.01%; Life Technologies), with pH adjusted to 7.4 and osmolarity of 290–300 mOsm. Recorded neurons were maintained at a holding potential of −65 mV.

Cultured neurons. Recordings were performed from cultured spinal cord neurons at 14–18 d in vitro at room temperature. Patch pipettes (4–6 MΩ) were filled with an internal solution containing 140 mM CsCl, 10 mM EGTA, 1 mM BAPTA, 1 mM MgCl$_2$, 4 mM Mg-ATP, 10 mM Hepes, and 5 mM QX314, adjusted to pH 7.4. Spontaneous currents were recorded at a holding potential of −60 mV. Neurons were continuously perfused with an external solution containing 137 mM NaCl, 5 mM KCl, 2 mM CaCl$_2$, 1 mM MgCl$_2$, 20 mM glucose, and 10 mM Hepes, pH 7.4. Spontaneous synaptic currents were detected using the Clampfit template procedure. In brief, for each cell, a sliding template was created by averaging 15–20 synaptic events, and detection of synaptic currents was done on the basis of closeness of fit to the sliding template. Overlapping events were excluded from amplitude analysis.

Acquisitions were performed using Clampex 10 software (Molecular Devices) connected to a Multiclamp 700B amplifier (Molecular Devices) via a Digidata 1440A digitizer (Molecular Devices). Voltage clamp data were filtered at 2 kHz and digitized at 10 kHz. The frequencies and amplitudes of inhibitory PSCs were analyzed with Clampfit (Axon Instruments).

All recordings were made in the presence of 6-cyano-7-nitroquinoxaline-2,3-dione (5 µM; Tocris) and D2-amino-5-phosphonovaleric acid (50 µM; Tocris). Selective antagonists were then used to block glycine receptors (strychnine hydrochloride; 0.5 µM) and GABA$_A$Rs (gabazine; SR95531; 5 µM; Tocris).

Cell-surface biotinylation assay

Cultured cells were incubated with biotin reagent (1 mg/ml NHS-SS-Biotin; Pierce), and unbound biotin was quenched with Dulbecco's PBS supplemented with 50 mM glycine, 0.8 mM CaCl$_2$, and 0.5 mM MgCl$_2$ at a pH level of 7.4. After lysing the cells with 1% Triton X-100 (wt/vol) in Tris buffer plus 2 mM EDTA and 2,000 U/ml benzonase (Merck), cleared Triton X-100 extracts were collected (10,000 g; 15 min) and mixed with neutravidin beads (Pierce) at 4°C. Immunoprecipitated and biotinylated proteins were separated by SDS-PAGE followed by immunoblotting with mAb4a antibody (1:500) or goat anti-GABA$_A$R γ2 (1:200; Santa Cruz Biotechnology). HRP-coupled secondary antibodies were used at 1:10,000. Proteins were visualized using an ECL and Amersham kit (Roche). For quantifications, the surface level of receptors was normalized to the corresponding level of protein detected in the immunoprecipitation fraction.

Single-particle tracking

All single-particle tracking experiments were performed in dissociated cultured cells. Cells were incubated with primary antibodies targeting extracellular epitopes of synaptic receptors. Cells were then incubated with anti–rabbit biotinylated secondary antibody fragment F(ab')2 (Jackson Immunoresearch) and then incubated with streptavidin-coated QDs emitting at 655 nm (0.2–0.3 nM; Invitrogen). Cells were

imaged within 30 to 40 min at 37°C using an IX70 inverted microscope (Olympus). QD movements were recorded at 13 Hz for 500 consecutive frames. QD trajectories were classified as synaptic when they colocalized with mRFP–gephyrin clusters. Only trajectories with >15 consecutive points were kept for quantitative analysis. Analyses were performed as described previously (Hennekinne et al., 2013). Synaptic dwell time was calculated as the time spent at synapses over the number of exits from synapses. Stable QD receptors were defined as a population remaining for the whole duration of the recording at mRFP–gephyrin–positive loci. Swapping QD receptor transition frequencies were calculated between each frame (sliding window of 75 ms) and normalized with the amount of synapses detected in the recorded field. The explored area of each trajectory was defined as the mean square displacement of the trajectory for a time interval between 1 and 1.5 s (Renner et al., 2009). The area was defined as synaptic when it colocalized with gephyrin-positive pixels.

Statistical analyses

Statistical analyses were performed using R (http://cran.r-project.org/), MATLAB (The Mathworks), and PRISM. Cumulative distributions were tested using the two-sample Kolmogorov-Smirnov test. Differences in mean values were tested using the Mann-Whitney test unless specified. Normality of the distributions was determined using the one-sample Kolmogorov-Smirnov test. For experiments performed in cultures, n is indicative of independent cultures. For experiments performed in organotypic slices or in animals, n is indicative of independent animals.

Online supplemental material

Fig. S1 shows that the short-term stimulation of microglia differentially decreases the synaptic accumulation of GlyR and GABA$_A$R in organotypic slices and dissociated cultured cells. Fig. S2 shows that microglia modulate the lateral diffusion parameters of synaptic but not extrasynaptic GlyR α1 and GABA$_A$R γ2. Fig. S3 (A and B) shows that the adaptive plastic regulation of GlyR is modulated by microglia in dissociated cultures. Fig. S4 shows that depletion of microglia by saporin is efficient and does not induce major alteration of inhibitory synapse proportion and density. Fig. S5 shows that EP2 receptor expression is neuronal and that blocking its function prevents the modulation of GlyR by LPS and 4AP in dissociated cultures.

References

Ahmadi, S., S. Lipross, W.L. Neuhuber, and H.U. Zeilhofer. 2002. PGE(2) selectively blocks inhibitory glycinergic neurotransmission onto rat superficial dorsal horn neurons. *Nat. Neurosci.* 5:34–40. http://dx.doi.org /10.1038/nn778

Bannai, H., S. Lévi, C. Schweizer, M. Dahan, and A. Triller. 2006. Imaging the lateral diffusion of membrane molecules with quantum dots. *Nat. Protoc.* 1:2628–2634. http://dx.doi.org/10.1038/nprot.2006.429

Basbaum, A.I., D.M. Bautista, G. Scherrer, and D. Julius. 2009. Cellular and molecular mechanisms of pain. *Cell.* 139:267–284. http://dx.doi.org/10 .1016/j.cell.2009.09.028

Béchade, C., Y. Cantaut-Belarif, and A. Bessis. 2013. Microglial control of neuronal activity. *Front. Cell. Neurosci.* 7:32. http://dx.doi.org/10.3389 /fncel.2013.00032

Berta, T., C.-K. Park, Z.-Z. Xu, R.-G. Xie, T. Liu, N. Lü, Y.-C. Liu, and R.-R. Ji. 2014. Extracellular caspase-6 drives murine inflammatory pain via microglial TNF-α secretion. *J. Clin. Invest.* 124:1173–1186. http://dx.doi .org/10.1172/JCI72230

Bilak, M., L. Wu, Q. Wang, N. Haughey, K. Conant, C. St Hillaire, and K. Andreasson. 2004. PGE2 receptors rescue motor neurons in a model of amyotrophic lateral sclerosis. *Ann. Neurol.* 56:240–248. http://dx.doi .org/10.1002/ana.20179

Broom, D.C., T.A. Samad, T. Kohno, I. Tegeder, G. Geisslinger, and C.J. Woolf. 2004. Cyclooxygenase 2 expression in the spared nerve injury model of neuropathic pain. *Neuroscience.* 124:891–900. http://dx.doi.org/10.1016 /j.neuroscience.2004.01.003

Chakravarty, S., and M. Herkenham. 2005. Toll-like receptor 4 on nonhematopoietic cells sustains CNS inflammation during endotoxemia, independent of systemic cytokines. *J. Neurosci.* 25:1788–1796. http://dx .doi.org/10.1523/JNEUROSCI.4268-04.2005

Chamak, B., A. Dobbertin, and M. Mallat. 1995. Immunohistochemical detection of thrombospondin in microglia in the developing rat brain. *Neuroscience.* 69:177–187. http://dx.doi.org/10.1016/0306-4522(95)00236-C

Charrier, C., P. Machado, R.Y. Tweedie-Cullen, D. Rutishauser, I.M. Mansuy, and A. Triller. 2010. A crosstalk between β1 and β3 integrins controls glycine receptor and gephyrin trafficking at synapses. *Nat. Neurosci.* 13:1388–1395. http://dx.doi.org/10.1038/nn.2645

Chen, Z., W. Jalabi, W. Hu, H.-J. Park, J.T. Gale, G.J. Kidd, R. Bernatowicz, Z.C. Gossman, J.T. Chen, R. Dutta, and B.D. Trapp. 2014. Microglial displacement of inhibitory synapses provides neuroprotection in the adult brain. *Nat. Commun.* 5:4486.

Choquet, D., and A. Triller. 2013. The dynamic synapse. *Neuron.* 80:691–703. http://dx.doi.org/10.1016/j.neuron.2013.10.013

Clark, A.K., D. Gruber-Schoffnegger, R. Drdla-Schutting, K.J. Gerhold, M. Malcangio, and J. Sandkühler. 2015. Selective activation of microglia facilitates synaptic strength. *J. Neurosci.* 35:4552–4570. http://dx.doi.org /10.1523/JNEUROSCI.2061-14.2015

Clasadonte, J., P. Poulain, N.K. Hanchate, G. Corfas, S.R. Ojeda, and V. Prevot. 2011. Prostaglandin E2 release from astrocytes triggers gonadotropin-releasing hormone (GnRH) neuron firing via EP2 receptor activation. *Proc. Natl. Acad. Sci. USA.* 108:16104–16109. http://dx.doi.org/10.1073 /pnas.1107533108

Costello, D.A., A. Lyons, S. Denieffe, T.C. Browne, F.F. Cox, and M.A. Lynch. 2011. Long term potentiation is impaired in membrane glycoprotein CD200-deficient mice: A role for Toll-like receptor activation. *J. Biol. Chem.* 286:34722–34732. http://dx.doi.org/10.1074/jbc.M111.280826

Coull, J.A.M., S. Beggs, D. Boudreau, D. Boivin, M. Tsuda, K. Inoue, C. Gravel, M.W. Salter, and Y. De Koninck. 2005. BDNF from microglia causes the shift in neuronal anion gradient underlying neuropathic pain. *Nature.* 438:1017–1021. http://dx.doi.org/10.1038/nature04223

Dahan, M., S. Lévi, C. Luccardini, P. Rostaing, B. Riveau, and A. Triller. 2003. Diffusion dynamics of glycine receptors revealed by single-quantum dot tracking. *Science.* 302:442–445. http://dx.doi.org/10.1126/science .1088525

Davalos, D., J. Grutzendler, G. Yang, J.V. Kim, Y. Zuo, S. Jung, D.R. Littman, M.L. Dustin, and W.-B. Gan. 2005. ATP mediates rapid microglial response to local brain injury in vivo. *Nat. Neurosci.* 8:752–758. http://dx .doi.org/10.1038/nn1472

De Simoni, A., N.J. Allen, and D. Attwell. 2008. Charge compensation for NAD PH oxidase activity in microglia in rat brain slices does not involve a proton current. *Eur. J. Neurosci.* 28:1146–1156. http://dx.doi.org/10.1111 /j.1460-9568.2008.06417.x

Ferrini, F., and Y. De Koninck. 2013. Microglia control neuronal network excitability via BDNF signalling. *Neural Plast.* 2013:429815. http://dx .doi.org/10.1155/2013/429815

Forselles, K.J., J. Root, T. Clarke, D. Davey, K. Aughton, K. Dack, and N. Pullen. 2011. In vitro and in vivo characterization of PF-04418948, a novel, potent and selective prostaglandin EP2 receptor antagonist. *Br. J. Pharmacol.* 164:1847–1856. http://dx.doi.org/10.1111/j.1476-5381 .2011.01495.x

Freund, T.F., and G. Buzsáki. 1996. Interneurons of the hippocampus. *Hippocampus.* 6:347–470. http://dx.doi.org/10.1002/(SICI)1098 -1063(1996)6:4<347::AID-HIPO1>3.0.CO;2-I

Hailer, N.P., J.D. Jarhult, and R. Nitsch. 1996. Resting microglial cells in vitro: Analysis of morphology and adhesion molecule expression in organotypic hippocampal slice cultures. *Glia.* 18:319–331. http://dx.doi.org/10.1002/ (SICI)1098-1136(199612)18:4<319::AID-GLIA3>3.0.CO;2-S

Hanus, C., M.-V. Ehrensperger, and A. Triller. 2006. Activity-dependent movements of postsynaptic scaffolds at inhibitory synapses. *J. Neurosci.* 26:4586–4595. http://dx.doi.org/10.1523/JNEUROSCI.5123-05.2006

Harvey, R.J., U.B. Depner, H. Wässle, S. Ahmadi, C. Heindl, H. Reinold, T.G. Smart, K. Harvey, B. Schütz, O.M. Abo-Salem, et al. 2004. GlyR α3: An essential target for spinal PGE2-mediated inflammatory pain sensitization. *Science.* 304:884–887. http://dx.doi.org/10.1126/science .1094925

Hellwig, S., A. Heinrich, and K. Biber. 2013. The brain's best friend: Microglial neurotoxicity revisited. *Front. Cell. Neurosci.* 7:71. http://dx.doi.org/10 .3389/fncel.2013.00071

Hennekinne, L., S. Colasse, A. Triller, and M. Renner. 2013. Differential control of thrombospondin over synaptic glycine and AMPA receptors in spinal cord neurons. *J. Neurosci.* 33:11432–11439. http://dx.doi.org/10.1523/ JNEUROSCI.5247-12.2013

Holm, T.H., D. Draeby, and T. Owens. 2012. Microglia are required for astroglial Toll-like receptor 4 response and for optimal TLR2 and TLR3 response. *Glia.* 60:630–638. http://dx.doi.org/10.1002/glia.22296

Ikeda-Matsuo, Y., Y. Ikegaya, N. Matsuki, S. Uematsu, S. Akira, and Y. Sasaki. 2005. Microglia-specific expression of microsomal prostaglandin E2 synthase-1 contributes to lipopolysaccharide-induced prostaglandin E2 production. *J. Neurochem.* 94:1546–1558. http://dx.doi.org/10.1111/j .1471-4159.2005.03302.x

Ji, R.-R., Z.-Z. Xu, and Y.-J. Gao. 2014. Emerging targets in neuroinflammation-driven chronic pain. *Nat. Rev. Drug Discov.* 13:533–548. http://dx.doi.org /10.1038/nrd4334

Jiang, J., and R. Dingledine. 2013. Prostaglandin receptor EP2 in the crosshairs of anti-inflammation, anti-cancer, and neuroprotection. *Trends Pharmacol. Sci.* 34:413–423. http://dx.doi.org/10.1016/j.tips.2013.05.003

Kilman, V., M.C.W. van Rossum, and G.G. Turrigiano. 2002. Activity deprivation reduces miniature IPSC amplitude by decreasing the number of postsynaptic GABA(A) receptors clustered at neocortical synapses. *J. Neurosci.* 22:1328–1337.

Kreutzberg, G.W. 1996. Microglia: A sensor for pathological events in the CNS. *Trends Neurosci.* 19:312–318. http://dx.doi.org/10.1016/0166 -2236(96)10049-7

Lagache, T., N. Sauvonnet, L. Danglot, and J.-C. Olivo-Marin. 2015. Statistical analysis of molecule colocalization in bioimaging. *Cytometry A.* 87:568– 579. http://dx.doi.org/10.1002/cyto.a.22629

Lehnardt, S., L. Massillon, P. Follett, F.E. Jensen, R. Ratan, P.A. Rosenberg, J.J. Volpe, and T. Vartanian. 2003. Activation of innate immunity in the CNS triggers neurodegeneration through a Toll-like receptor 4-dependent pathway. *Proc. Natl. Acad. Sci. USA.* 100:8514–8519. http://dx.doi.org /10.1073/pnas.1432609100

Lévi, S., C. Schweizer, H. Bannai, O. Pascual, C. Charrier, and A. Triller. 2008. Homeostatic regulation of synaptic GlyR numbers driven by lateral diffusion. *Neuron.* 59:261–273. http://dx.doi.org/10.1016/j.neuron.2008 .05.030

Li, Y., X.-F. Du, C.-S. Liu, Z.-L. Wen, and J.-L. Du. 2012. Reciprocal regulation between resting microglial dynamics and neuronal activity in vivo. *Dev. Cell.* 23:1189–1202. http://dx.doi.org/10.1016/j.devcel.2012.10.027

Liang, X., Q. Wang, J. Shi, L. Lokteva, R.M. Breyer, T.J. Montine, and K. Andreasson. 2008. The prostaglandin E2 EP2 receptor accelerates

disease progression and inflammation in a model of amyotrophic lateral sclerosis. *Ann. Neurol.* 64:304–314. http://dx.doi.org/10.1002/ana.21437

Murphy-Royal, C., J.P. Dupuis, J.A. Varela, A. Panatier, B. Pinson, J. Baufreton, L. Groc, and S.H.R. Oliet. 2015. Surface diffusion of astrocytic glutamate transporters shapes synaptic transmission. *Nat. Neurosci.* 18:219–226. http://dx.doi.org/10.1038/nn.3901

Nimmerjahn, A., F. Kirchhoff, and F. Helmchen. 2005. Resting microglial cells are highly dynamic surveillants of brain parenchyma in vivo. *Science.* 308:1314–1318. http://dx.doi.org/10.1126/science.1110647

Oliveira, A.L., S. Thams, O. Lidman, F. Piehl, T. Hökfelt, K. Kärre, H. Lindå, and S. Cullheim. 2004. A role for MHC class I molecules in synaptic plasticity and regeneration of neurons after axotomy. *Proc. Natl. Acad. Sci. USA.* 101:17843–17848. http://dx.doi.org/10.1073/pnas.0408154101

Parkhurst, C.N., G. Yang, I. Ninan, J.N. Savas, J.R. Yates III, J.J. Lafaille, B.L. Hempstead, D.R. Littman, and W.-B. Gan. 2013. Microglia promote learning-dependent synapse formation through brain-derived neurotrophic factor. *Cell.* 155:1596–1609. http://dx.doi.org/10.1016/j.cell.2013.11.030

Pascual, O., S. Ben Achour, P. Rostaing, A. Triller, and A. Bessis. 2012. Microglia activation triggers astrocyte-mediated modulation of excitatory neurotransmission. *Proc. Natl. Acad. Sci. USA.* 109:E197–E205. http://dx.doi.org/10.1073/pnas.1111098109

Pribiag, H., and D. Stellwagen. 2013. TNF-α downregulates inhibitory neurotransmission through protein phosphatase 1-dependent trafficking of GABA(A) receptors. *J. Neurosci.* 33:15879–15893. http://dx.doi.org/10.1523/JNEUROSCI.0530-13.2013

Ragozzino, D., S. Di Angelantonio, F. Trettel, C. Bertollini, L. Maggi, C. Gross, I.F. Charo, C. Limatola, and F. Eusebi. 2006. Chemokine fractalkine/CX3CL1 negatively modulates active glutamatergic synapses in rat hippocampal neurons. *J. Neurosci.* 26:10488–10498. http://dx.doi.org/10.1523/JNEUROSCI.3192-06.2006

Ransohoff, R.M., and A.E. Cardona. 2010. The myeloid cells of the central nervous system parenchyma. *Nature.* 468:253–262. http://dx.doi.org/10.1038/nature09615

Reinold, H., S. Ahmadi, U.B. Depner, B. Layh, C. Heindl, M. Hamza, A. Pahl, K. Brune, S. Narumiya, U. Müller, and H.U. Zeilhofer. 2005. Spinal inflammatory hyperalgesia is mediated by prostaglandin E receptors of the EP2 subtype. *J. Clin. Invest.* 115:673–679. http://dx.doi.org/10.1172/JCI23618

Ren, J., J.H. Ye, and J.J. McArdle. 1998. cAMP-dependent protein kinase modulation of glycine-activated chloride current in neurons freshly isolated from rat ventral tegmental area. *Brain Res.* 811:71–78. http://dx.doi.org/10.1016/S0006-8993(98)00959-7

Renner, M., D. Choquet, and A. Triller. 2009. Control of the postsynaptic membrane viscosity. *J. Neurosci.* 29:2926–2937. http://dx.doi.org/10.1523/JNEUROSCI.4445-08.2009

Renner, M., P.N. Lacor, P.T. Velasco, J. Xu, A. Contractor, W.L. Klein, and A. Triller. 2010. Deleterious effects of amyloid beta oligomers acting as an extracellular scaffold for mGluR5. *Neuron.* 66:739–754. http://dx.doi.org/10.1016/j.neuron.2010.04.029

Rogers, J.T., J.M. Morganti, A.D. Bachstetter, C.E. Hudson, M.M. Peters, B.A. Grimmig, E.J. Weeber, P.C. Bickford, and C. Gemma. 2011. CX3CR1 deficiency leads to impairment of hippocampal cognitive function and synaptic plasticity. *J. Neurosci.* 31:16241–16250. http://dx.doi.org/10.1523/JNEUROSCI.3667-11.2011

Roumier, A., C. Béchade, J.-C. Poncer, K.-H. Smalla, E. Tomasello, E. Vivier, E.D. Gundelfinger, A. Triller, and A. Bessis. 2004. Impaired synaptic function in the microglial KARAP/DAP12-deficient mouse. *J. Neurosci.* 24:11421–11428. http://dx.doi.org/10.1523/JNEUROSCI.2251-04.2004

Saijo, K., B. Winner, C.T. Carson, J.G. Collier, L. Boyer, M.G. Rosenfeld, F.H. Gage, and C.K. Glass. 2009. A Nurr1/CoREST pathway in microglia and astrocytes protects dopaminergic neurons from inflammation-induced death. *Cell.* 137:47–59. http://dx.doi.org/10.1016/j.cell.2009.01.038

Samad, T.A., K.A. Moore, A. Sapirstein, S. Billet, A. Allchorne, S. Poole, J.V. Bonventre, and C.J. Woolf. 2001. Interleukin-1β-mediated induction of Cox-2 in the CNS contributes to inflammatory pain hypersensitivity. *Nature.* 410:471–475. http://dx.doi.org/10.1038/35068566

Shrivastava, A.N., V. Redeker, N. Fritz, L. Pieri, L.G. Almeida, M. Spolidoro, T. Liebmann, L. Bousset, M. Renner, C. Léna, et al. 2015. α-synuclein assemblies sequester neuronal α3-Na+/K+-ATPase and impair Na+ gradient. *EMBO J.* 34:2408–2423. http://dx.doi.org/10.15252/embj.201591397

Specht, C.G., N. Grünewald, O. Pascual, N. Rostgaard, G. Schwarz, and A. Triller. 2011. Regulation of glycine receptor diffusion properties and gephyrin interactions by protein kinase C. *EMBO J.* 30:3842–3853. http://dx.doi.org/10.1038/emboj.2011.276

Stellwagen, D., and R.C. Malenka. 2006. Synaptic scaling mediated by glial TNF-α. *Nature.* 440:1054–1059. http://dx.doi.org/10.1038/nature04671

Tremblay, M.-È., R.L. Lowery, and A.K. Majewska. 2010. Microglial interactions with synapses are modulated by visual experience. *PLoS Biol.* 8:e1000527. http://dx.doi.org/10.1371/journal.pbio.1000527

Tremblay, M.-È., B. Stevens, A. Sierra, H. Wake, A. Bessis, and A. Nimmerjahn. 2011. The role of microglia in the healthy brain. *J. Neurosci.* 31:16064–16069. http://dx.doi.org/10.1523/JNEUROSCI.4158-11.2011

Wake, H., A.J. Moorhouse, S. Jinno, S. Kohsaka, and J. Nabekura. 2009. Resting microglia directly monitor the functional state of synapses in vivo and determine the fate of ischemic terminals. *J. Neurosci.* 29:3974–3980. http://dx.doi.org/10.1523/JNEUROSCI.4363-08.2009

Wang, Y., M. Cella, K. Mallinson, J.D. Ulrich, K.L. Young, M.L. Robinette, S. Gilfillan, G.M. Krishnan, S. Sudhakar, B.H. Zinselmeyer, et al. 2015. TREM2 lipid sensing sustains the microglial response in an Alzheimer's disease model. *Cell.* 160:1061–1071. http://dx.doi.org/10.1016/j.cell.2015.01.049

Zhao, P., S.G. Waxman, and B.C. Hains. 2007. Extracellular signal-regulated kinase-regulated microglia-neuron signaling by prostaglandin E2 contributes to pain after spinal cord injury. *J. Neurosci.* 27:2357–2368. http://dx.doi.org/10.1523/JNEUROSCI.0138-07.2007